Journal of Materials Chemistry

Cite this: J. Mater. Chem., 2012, 22, 7387

www.rsc.org/materials

PAPER

Tetraphenylethenyl-modified perylene bisimide: aggregation-induced red emission, electrochemical properties and ordered microstructures†

Qiuli Zhao,[a] Shuang Zhang,[a] Yi Liu,[a] Ju Mei,[a] Sijie Chen,[b] Ping Lu,[c] Anjun Qin,[a] Yuguang Ma,[c] Jing Zhi Sun*[a] and Ben Zhong Tang*[ab]

Received 15th December 2011, Accepted 27th January 2012
DOI: 10.1039/c2jm16613e

Perylene bisimides (PBIs) are one class of the most explored organic fluorescent materials due to their high fluorescence quantum efficiency, electron transport behaviour, and ready to form well-tailored supramolecular structures. However, they suffer from heavy aggregation-caused quenching (ACQ) effect which has greatly limited their potential applications. We successfully tackle this problem by chemical modification of the PBI core with two tetraphenylethene (TPE) moieties at the bay positions. This modification resulted in a pronounced fluorescence red-shift (over 120 nm) and rendered the derivatives (1,6-/1,7-DTPEPBI) with evident aggregation-induced emission (AIE) behaviour. Both 1,6-DTPEPBI and 1,7-DTPEPBI emit bright red fluorescence in the solid state. The fluorescence quantum efficiency of the aggregates of 1,7-DTPEPBI ($\Phi_{F,\ solid} = 29.7\%$, formed in a hexane/dichloromethane mixture, $f_h = 90\%$) is about 424 times higher than that in dichloromethane solution ($\Phi_{F,\ solut} = 0.07\%$). Electrochemical investigation results indicated that 1,7-DTPEPBI sustained the intrinsic n-type semiconductivity of PBI moiety. In addition, morphological inspection demonstrated that 1,7-DTPEPBI molecules easily form well-organized microstructures despite the linkage of the PBI core with bulky TPE moieties.

Introduction

Perylene bisimides (PBIs) are one kind of the most investigated organic dyes that have found promising applications as active components in organic light harvesting systems, n-type channel field effect transistors, fluorescent emitters and biosensors, and the construction of self-assembling nanostructures.[1–4] PBIs demonstrate near-unity fluorescence (FL) quantum yields in dilute solutions, but in poor solvents or in solid state, PBI molecules are prone to form aggregates, which leads to FL quenching because of the attractive dipole–dipole interactions and/or effective inter-molecular π–π stacking. This effect is termed aggregation-caused quenching (ACQ).[5] It is of great significance to make PBI-based dyes efficiently emit in the solid state. A wise strategy is to modify the PBI-based dyes by attaching bulky substituents onto the chromophore to restrict the intermolecular π–π stacking and to hinder the intermolecular electronic coupling and the resulting PBIs exhibit desirable quantum efficiency of light emission.[6]

Tetraphenylethene (TPE) has a bulky size and propeller shape. It has been found that TPE and its derivatives are non-emissive in solutions but highly emissive by aggregate formation. This phenomenon is termed "aggregation-induced emission" (AIE).[5,7,8] Recently, we have demonstrated that combining TPE moieties with classical fluorogens such as naphthalene, quinoline, anthracene, phenanthracene, carbazole, and pyrene can convert these conventional dyes into efficient solid-state emitters (Chart 1).[9] Based on these achievements, it is a rational assumption to tackle the notorious ACQ behavior of PBIs by means of modifying PBI with TPE moieties. But for the expected PBI-TPE dyads, there still are unknowns and challenges. Firstly, the fluorogens described in literature are small planar aromatics (*e.g.* naphthalene, anthracene, phenanthracene, and pyrene).[9] Can it be workable to convert larger planar PBI from a typical ACQ to an AIE by attaching TPE moieties to the PBI core?

[a]*MOE Key Laboratory of Macromolecular Synthesis and Functionalization, Institute of Biomedical Macromolecules, Department of Polymer Science and Engineering, Zhejiang University, Hangzhou, 310027, China. E-mail: sunjz@zju.edu.cn; Fax: 86-571-87953734*
[b]*Department of Chemistry and State Key Laboratory of Molecular NeuroScience, The Hong Kong University of Science & Technology, Clear Water Bay, Kowloon, Hong Kong, China. E-mail: tangbenz@ust.hk; Fax: + 852-2358-7375*
[c]*State Key Laboratory of Supramolecular Structure and Materials, Jilin University, Changchun, 130012, China*

† Electronic Supplementary Information (ESI) available: ^{1}H and ^{13}C NMR spectra of 1,6-/1,7-DTPEPBI, fluorescence spectra of 1,7-DTPEPBI in different non-solvent/solvent mixtures such as methanol/DCM and water/THF, fluorescence spectrum of the solid film of 1,7-DTPEPBI, fluorescence spectra of 1,6-DTPEPBI in hexane/DCM mixtures with different hexane contents, typical SEM images of 1,7-DTPEPBI aggregates formed in different conditions, polarized optical microscopic and confocal fluorescence images of the microstructures formed by 1,7-DTPEPBI and 1,7-DBrPBI. See DOI: 10.1039/c2jm16613e

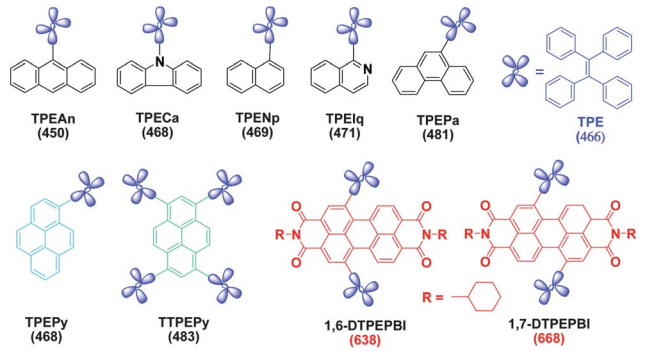

Chart 1 Chemical structures of 1,6-DTPEPBI and 1,7-DTPEPBI, as well as a series of classical fluorogens modified with tetraphenylethene (TPE) moiety/moieties. The numbers in bracket are the maximum of the fluorescence spectrum of the corresponding solid film.

Secondly, PBI and TPE are n- and p-type organic semiconductors, respectively. What is the effect of linking TPE moieties to PBI on the semiconductive behavior of the derived dyad? And thirdly, PBIs are prone to self-assemble into ordered supramolecular structures. It is an important issue to know the effects of attaching twisted and bulky TPE moieties onto the PBI core on the assembling behavior of the derived molecules. Herein, we report the design and synthesis of novel PBI derivatives decorated with TPE moieties (see Chart 1, 1,6-DTPEPBI and 1,7-DTPEPBI), and demonstrate our efforts to address the above-mentioned issues by using them as representative compounds.

Results and discussion

Synthesis of 1,6-DTPEPBI and 1,7-DTPEPBI

The synthetic route to 1,6-/1,7-DTPEPBI is shown in Scheme 1. The detailed procedures for the syntheses of the intermediates and final products are described in the experimental section and Electronic Supplementary Information (ESI).† In brief, the bromination of 3,4,9,10-perylenetetracarboxylic dianhydride (PTCDA) was according to ref. 10 and a mixture of 1,6-dibromo-3,4,9,10-perylenetetracarboxylic dianhydride (1,6-DBrPTCDA) and 1,7-dibromo-3,4,9,10-perylenetetracarboxylic dianhydride (1,7-DBrPTCDA) was obtained. It was very difficult to separate the two isomers, thus we proceeded to the imidization reaction without purification. The reaction afforded a mixture of *N*,*N*′-cyclohexamethyl-1,6-dibromo-3,4,9,10-perylene tetracarboxylic bisimide (1,6-DBrPBI) and *N*,*N*′-cyclohexamethyl-1,7-dibromo-3,4,9,10-perylene tetracarboxylic bisimide (1,7-DBrPBI). The intermediate of 4-(1,2,2-triphenyvinyl) phenylboronic acid (TPVPBC) was prepared according to our previously published procedures (Scheme S1†).[9a] Suzuki coupling TPVPBC with 1,6-DBrPBI and 1,7-DBrPBI catalyzed by $Pd(PPh_3)_4$ gave rise to a mixture of [*N*,*N*′-dicyclohexyl-1,6-bis(4′-(1′,2′,2′-triphenyl) vinyl)phenylperylene-3,4:9,10-tetrcarboxylic bisimide] (1,6-DTPEPBI) and [*N*,*N*′-dicyclohexyl-1,7-bis(4′-(1′,2′,2′-triphenyl) vinyl)phenylperylene-3,4:9,10-tetracarboxylic bisimide] (1,7-DTPEPBI) in high yield. Fortunately, the final products 1,6-DTPEPBI and 1,7-DTPEPBI can be completely separated by simple column chromatography.

Generally, the full separation of isomers of 1,6- and 1,7-substituted PBIs is a challenging work. Up to now, there are only few reports of the isolation and characterization of 1,6-/1,7-disubstituted PBIs.[11] In the present case, the two regioisomers 1,7-DTPEPBI and 1,6-DTPEPBI were easily separated by conventional column chromatography using DCM/petroleum ether (2 : 3 by volume) as eluent (for the characterization data see experimental section and ESI† for details). This can be associated with the fact that the substitution of bromides at 1,6-/1,7-positions with TPEs renders 1,7-DTPEPBI and 1,6-DTPEPBI with enhanced differences in molecular shape and symmetry. The separation result revealed that the ratio of 1,7-DTPEPBI to 1,6-DTPEPBI is 4 : 1, indicating that 1,7-DTPEPBI is the dominant product. Here, we purified 1,7-DTPEPBI from the mixture of the two regioisomers, and mainly studied the properties of 1,7-DTPEPBI. Both 1,6-DTPEPBI and 1,7-DTPEPBI have good solubility in common organic solvents such as tetrahydrofuran (THF), chloroform, and dichloromethane (DCM), but poor in hexane, methanol and ethanol. The structures of the intermediates and products were characterized with multiple spectroscopic techniques and satisfactory data were obtained (experimental section and ESI†).

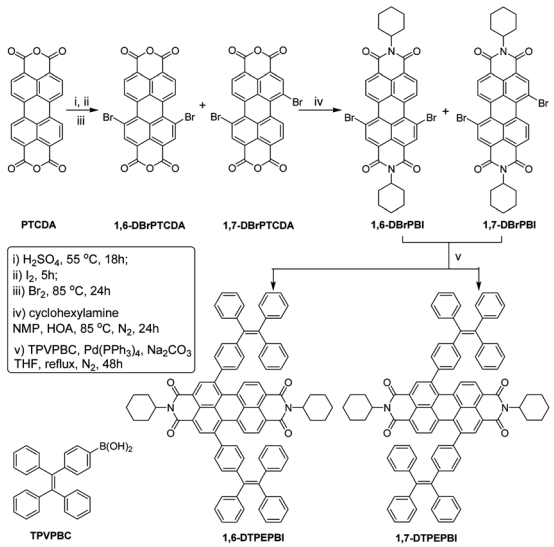

Scheme 1 Synthetic route to 1,6-DTPEPBI and 1,7-DTPEPBI.

Fluorescent behavior of 1,6-DTPEPBI and 1,7-DTPEPBI

PBI derivatives usually emit intense fluorescence in solution, but become faintly or even non-emissive in aggregated or solid states.[3,4,12] This was confirmed again by the emission behavior of 1,6-DBrPBI and 1,7-DBrPBI in water/THF mixtures with different water fractions (f_w). The fluorescence spectrum of 1,7-DBrPBI in THF solution shows a maximum at 545 nm and a pronounced shoulder around 580 nm. With addition of water, the emission intensity decreases. When $f_w < 50\%$, the change in emission intensity is rather small; when $50\% \leq f_w < 80\%$, the emission intensity decreases drastically; and when $f_w \geq 80\%$, the emission spectra are nearly parallel to the abscissa (Fig. 1B). The photographs displaying the emission change are shown in Fig. 1C. The decrease of emission intensity with the increasing of

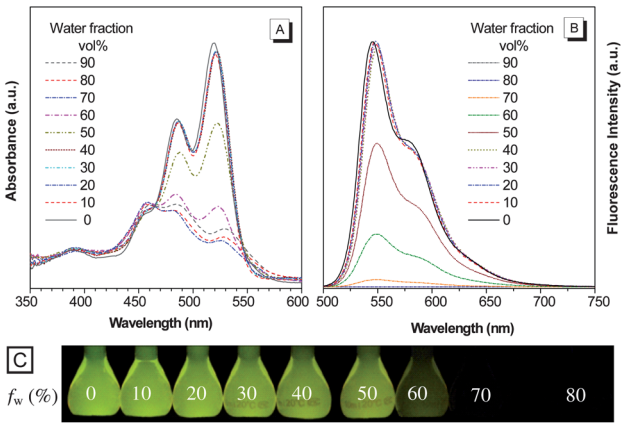

Fig. 1 (A) Absorption spectra of 1,7-DBrPBI in H_2O/THF mixtures with different water fractions (f_W, by volume%). (B) Fluorescence spectra of 1,7-DBrPBI in H_2O/THF mixtures with different f_W values. Excitation wavelength: 485 nm. (C) Images showing the fluorescence of 1,7-DBrPBI in H_2O/THF mixtures with different f_W values taken under UV illumination. Excitation wavelength: 365 nm. [1,7-DBrPBI] = 10^{-5} M.

f_w can be ascribed to the formation of aggregates in the mixtures of water/THF, which is due to the π–π electronic coupling between perylene chromophores. Absorption spectra in Fig. 1A give convincing evidence. The absorption bands at 520 and 485 nm are assigned to the 0–0 and 0–1 electronic transitions of the PBI chromophore. They decreased gradually with the increasing of f_w. Moreover, the relative intensity of 0–0 and 0–1 bands reverses as $f_w \geq 60\%$. According to literature, such a feature change indicates strong molecular aggregation induced by π–π stacking.[4,12] Furthermore, the absorption data in Fig. 1A also indicate the precipitation upon addition of water since the overall absorption band is decreasing and could account for the decrease in fluorescence as shown for 1,7-DBrPBI in the same solvent mixture. Based on the analyses of the absorption and emission spectra, 1,7-DBrPBI is assigned to an ACQ molecule.

In contrast, 1,7-DTPEPBI is non-emissive when dissolved in good solvents, such as THF and dichloromethane (DCM),

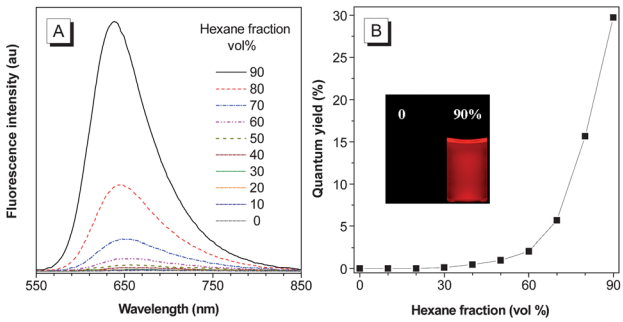

Fig. 2 (A) Fluorescence spectra of 1,7-DTPEPBI in hexane/DCM (dichloromethane) mixtures with different hexane fractions (f_h, by volume%). Excitation wavelength: 452 nm. (B) Quantum yield [estimated by using Rhodamine B as standard (Φ_F = 70% in ethanol)] of 1,7-DTPEPBI in hexane/DCM mixtures with different f_h values. Inset: fluorescence images of 1,7-DTPEPBI in hexane/DCM mixtures with f_h values of 0 and 90%, respectively. The photographs were taken under UV illumination. Excitation wavelength: 365 nm. [1,7-DTPEPBI] = 10^{-5} M.

a hydrophilic and a hydrophobic solvent, respectively (Fig. 2 and S3, S4†). However, when enough non-solvent (hexane, methanol or water) was added into the solution, the resultant mixture emitted evidently enhanced fluorescence. We investigated the fluorescence behavior of 1,7-DTPEPBI in three different non-solvent/solvent systems, which were hexane/DCM (hydrophobic/hydrophobic), methanol/DCM (hydrophilic/hydrophobic) and water/THF (hydrophilic/hydrophilic). In hexane/DCM, the fluorescence spectra of 1,7-DTPEPBI in mixed solvents are nearly parallel to the abscissa as $f_h < 40\%$ (f_h, the percentage volume fraction of hexane in the hexane/DCM mixture). However, the emission is gradually enhanced when $f_h > 40\%$ (Fig. 2A and B). When $I/I_0 - 1$ is calculated, it can be figured out that the emission intensity at $f_h = 90\%$ is over 530 times that at $f_h = 0$; where I_0 and I are the fluorescence intensities recorded for $f_h = 0$ and another hexane percentage, respectively. Since hexane is a non-solvent of 1,7-DTPEPBI, containing enough hexane in the mixture would make the molecules insoluble and aggregates should form in the mixture. According to the well-accepted mechanism of the AIE phenomenon, in solution, the active intramolecular rotations of the multiple phenyl rotors in TPE around the PBI stators consume the excited energy and quench the fluorescence; while in aggregates, molecular stacking restricts the rotation of the phenyl rotors and induces the emission of the fluorescence.

Similar fluorescent behavior was observed for methanol/DCM and water/THF systems. In methanol/DCM mixtures, the fluorescence intensity of the mixtures was greatly enhanced when $f_m \geq 70\%$ (f_m, the percentage volume fraction of methanol in methanol/DCM). However, when f_m was over 80%, the fluorescence intensity decreased gradually (Fig. S3†). This phenomenon can be explained as follows. At high f_m value, 1,7-DTPEPBI molecules easily form larger aggregates, which precipitate quickly. Meanwhile, the formation of larger aggregates decreases the number of the emissive species in the mixture. The tendency to form large aggregates can be associated with the hydrophobic nature of 1,7-DTPEPBI molecules, which allows them to isolate when hydrophilic methanol is added into the mixture. In water/THF (hydrophilic/hydrophilic) mixtures, the precipitate can be quickly observed when f_w is only 40%. This made the fluorescence enhancement be lower than that observed in hexane/DCM and methanol/DCM systems The fluorescence intensity only showed very a limited increase when a large amount of water was introduced into the water/THF mixture (Fig. S4†). In this case, the large particles precipitated during the measurement, only those smaller ones in the suspension contributed to the emission. Such an observation suggests that the hydrophobic 1,7-DTPEPBI molecules had formed large aggregates, because both water and THF are hydrophilic solvents.

In the mixed solvents such as water/THF or methanol/DCM, when enough non-solvents ($f_w \geq 40\%$ or $f_m \geq 70\%$) were added, rather broad and red-shifted absorption bands were observed (Fig. S4A and S5†). Such feature changes are typical characteristics of *J*-aggregation.[3a,4,12,13] Moreover, the relative intensity of 0–0 and 0–1 bands reverses. These spectral changes indicated that 1,7-DTPEPBI molecules are arranged in slipped face-to-face fashion to form *J*-aggregates.[12,13]

The fluorescence quantum efficiencies (Φ_F) of 1,7-DTPEPBI was evaluated by using Rhodamine B as standard. In dilute

DCM solution, the $\Phi_{F,\ solut}$ of 1,7-DTPEPBI is only 0.07%, while in solid film, the $\Phi_{F,\ solid}$ becomes 6.3%, indicating an amplification factor ($\Phi_{F,\ solid}/\Phi_{F,\ solut}$) of 90. It is noticeable that the $\Phi_{F,\ solid}$ value of 1,7-DTPEPBI in solid film is close to the best data up to now obtained by introducing bulky substituents onto the fluorogens to prevent the molecules from strong intermolecular π–π interaction.[4,6] In a hexane/DCM mixture with f_h = 90%, Φ_F increases up to 29.7% and an amplification factor of 424.3 (Fig. 2B). As displayed in Fig. S6,† 1,6-DTPEPBI demonstrates identical fluorescent behavior in hexane/DCM mixtures. When f_h is higher than 50%, the fluorescence begins to elevate; when f_h is 90%, Φ_F increases to 22.8%, indicating an amplification factor of 326. Qualitatively, in methanol/DCM and water/THF mixed solvents, 1,7-DTPEPBI demonstrated fluorescent behavior similar to that in hexane/DCM mixtures (Fig. S3 and S4†). Quantitatively, the fluorescence amplification is not as high as that observed in the hexane/DCM system. Compared with the fluorescent behavior of other AIE active materials reported in literature,[7–9] we can conclude that both 1,6-DTPEPBI and 1,7-DTPEPBI are typical AIE active molecules.

In comparison of the fluorescence spectra of 1,7-DTPEPBI with those of 1,7-DBrPBI, another significant difference can be recognized. That is, the aggregates of 1,7-DTPEPBI formed in hexane/DCM, methanol/DCM and water/THF emit red fluorescence, and the emission peaks appear at 638, 668 and 693 nm, respectively. Meanwhile, the maximum of the fluorescence spectra for the solid film of 1,7-DTPEPBI also appears at 668 nm (Fig. S7†). As a comparison, the emission maximum for the powder of the 1,7-DBrPBI appears at 607 nm (Fig. S8†). The experiment data indicate that evident red-shifts of 31, 61 and 86 nm have been achieved in different aggregate states. This spectral shift means the modification of PBI with TPE moieties has transferred the emission from green to red. This is different from our previous observations for the decoration of naphthalene, anthracene, and pyrene with TPE moieties, in which only a small red-shift of emission spectra has been achieved. Even attachment of four TPE moieties to the pyrene core can only result in a fluorescent change from purple and blue (400 nm for pyrene monomer and 468 nm for excimer) to blue-greenish (483 nm) (see Chart 1).

Electronic structure

To get better understanding of the mechanism of the pronounced fluorescence red-shift, the electronic structure of 1,7-DTPEPBI is estimated by theoretical simulation and their molecular structures were optimized by the semi-empirical AM1 method. The calculation results reveal that the HOMO and LUMO of 1,7-DTPEPBI are localized predominately on the molecular skeleton of the central PBI moiety, just like its precursor 1,7-DBrPBI (Fig. 3A and S9†), while the TPE moieties have hardly contributed to the molecular orbital of 1,7-DTPEPBI. Meanwhile, the phenyls in the TPE units are arranged in a propeller-like shape (Fig. 3C). As a result, the remarkable red-shift fluorescence cannot be fully ascribed to the extended conjugation of PBI with TPE moieties. Based on the theoretical calculation, the twist angles of the two naphthalenoid moieties of 1,7-DBrPBI and 1,7-DTPEPBI are 24.10° and 12.05° (Fig. 3B and C), respectively,

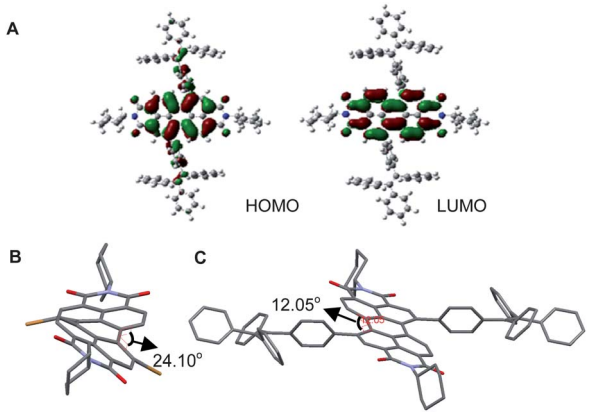

Fig. 3 (A) Molecular orbital amplitude plots of HOMO and LUMO energy levels of 1,7-DTPEPBI. (B) and (C) show the optimal structures of 1,7-DBrPBI and 1,7-DTPEPBI calculated by the semi-empirical AM1 method. The white, grey, blue, red, and scarlet balls represent H, C, N, O, and Br atoms, respectively. The H atoms are omitted for clarity.

which are nearly the same as reported in literature,[4e] and these results suggest that 1,7-DTPEPBI has a more planar configuration than 1,7-DBrPBI. This result may partially explain the observed large red-shift florescence of 1,7-DTPEPBI relative to 1,7-DBrPBI.

Since the electronic structure of 1,7-DTPEPBI is calculated to be dominated by the PBI core, it is expected that the n-type semiconductor behaviour will remain unchanged by the attachment of TPE moieties onto the 1,6-/1,7-positions of a PBI moiety. This has been confirmed by experiment results of cyclic-voltammetry measurements. In DCM solution, 1,7-DBrPBI shows two sets of single redox waves and the related first redox wave $E_{1/2}$ and ΔE_P values are 589 and 76 mV, respectively. 1,7-DTPEPBI shows similar redox behavior, its $E_{1/2}$ and ΔE_P values are 715 and 207 mV, respectively (Fig. 4). These results indicate that 1,7-DTPEPBI has the same electrochemical behavior as PBI and can be assigned to an n-type organic semiconductor.

Ordered microstructures

Owing to the strong π–π interaction between perylene cores, PBI derivatives are prone to assemble into ordered one-dimensional (1D) nanostructures such as wires, rods and belts. However, some investigation results demonstrated that the PBI derivatives with bulky substituents at the bay area (1,6-/1,7-positions) were

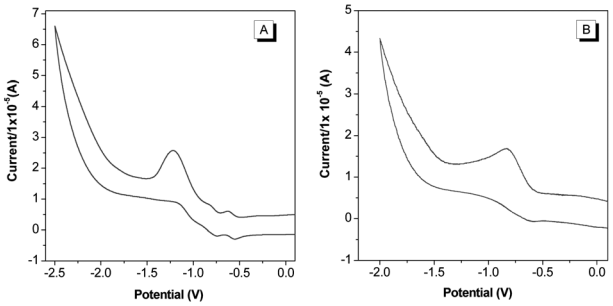

Fig. 4 Cyclic voltammograms of 1,7-DBrPBI (A) and 1,7-DTPEPBI (B) in dichloromethane containing 0.1 M Bu_4NPF_6.

difficult to form well-defined nanostructures due to the distorting π–π stacking.[14] TPE is a bulky substituent and has a propeller-like shape, thus the attachment of TPEs at the bay area of a PBI core may heavily distort the π–π stacking between the PBI units. Consequently, it seems that ordered nano/microstructures cannot be expected. To our surprise, however, we have found that 1,7-DTPEPBI can easily form micro-fibers in the mixtures of hexane/DCM, methanol/DCM and water/THF. The typical morphologies are displayed by the SEM images in Fig. 5 and S10–S12.† For example, in the mixture of methanol/DCM with f_m = 70%, 1,7-DTPEPBI molecules assembled into fibers with lengths of several tens of microns and diameters of 100–300 nanometres (Fig. 5A and the inset). Changing of the f_m value resulted in fibrils with similar morphologies (Fig. S10†). In the mixed solvent of water/THF, 1,7-DTPEPBI molecules could also assemble into micro-scale fibrils at different f_w values; an apparent difference can be found that the size of the micro-fibers is smaller than that observed in the mixture of methanol/DCM at the same volume fraction of non-solvent (Fig. 5B, the inset and S11†). These observations imply that 1,7-DTPEPBI keeps the intrinsic behaviour to form 1D microstructures. Thus it is reasonable to conceive that better organized 1D microstructures may be generated by adjusting the solvent or/and experiment condition. Indeed, we obtained well-ordered fibrils in other non-solvent/solvent mixtures (Fig. 5C, 5D and S11, S12†). As displayed in Fig. 5C, in the methanol/THF mixture with 90% methanol (by volume), micro-tapes with length of 50–200 micrometres and width about 100 micrometres have been formed. The inset demonstrates that microstructures have smooth surfaces and regular edges, indicating better organized 1D microstructures have formed. In Fig. 5D, we can find that fibrils with length of hundreds of micrometres with different diameters have been generated in the methanol/dioxane mixture with 80% methanol.

When slowly evaporating THF from the water/THF mixture, the f_w value increases gradually and 1,7-DTPEPBI molecules can assemble into higher ordered microstructures. As shown by Fig. 5E and the inset, fibrils with lengths of hundreds of micrometres and diameters of 100–200 nanometres are derived from the water/THF mixture at f_m = 40%. In fact, needle- and prism-like microstructures of 1,7-DTPEPBI can be obtained by slowly evaporating the solvent from its THF or DCM solution (Fig. 5F). The polarized optical microscopy (POM) images demonstrate evident anisotropic reflections, indicating that the fibrils and prism-like microstructures are crystals (Fig. 6A and B). Moreover, thanks to the AIE behaviour of 1,7-DTPEPBI, the microcrystals and micro-fibrils emit intense red fluorescence upon excitation with green light, as shown by the confocal fluorescence images in Fig. 6C, D and S13.† In contrast, the POM observation for a powder sample of DBrPBI only showed weak orange fluorescence during the confocal imaging measurement (Fig. S14A and S14B†). In addition, both of the

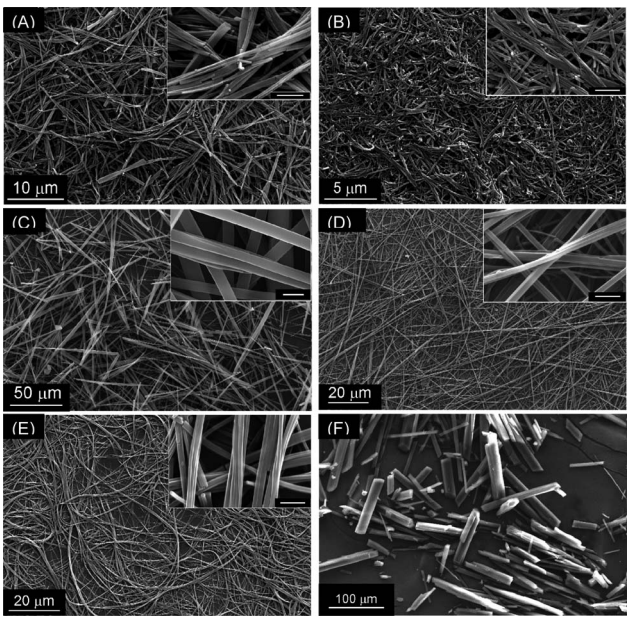

Fig. 5 (A)–(F): SEM images of the morphologies of the aggregates formed by 1,7-DTPEPBI molecules in different conditions. (A) In methanol/DCM mixture with a methanol fraction (f_m, by volume) of 70%. (B) In water/THF mixture with a water fraction (f_w, by volume) of 60%. (C) In methanol/THF mixture with a methanol fraction (f_m, by volume) of 90%. (D) In methanol/dioxane mixture with a methanol fraction (f_m, by volume) of 80%. (E) Fibrils formed by slowly evaporation of solvent from water/THF mixture with an f_w of 40%. (F) Rod- and prism-like microstructures formed by slow evaporation of 1,7-DTPEPBI THF solution. The scale bar shown in all of the insets is 1 μm. In all experiments, the concentration of 1,7-DTPEPBI is 10^{-5} M.

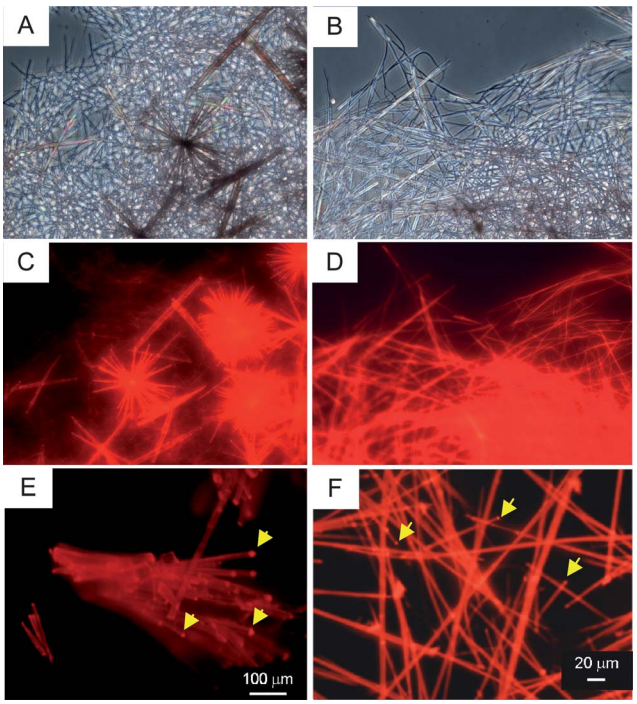

Fig. 6 Polarized optical microscopic images of the microcrystals obtained from a methanol/DCM mixture (A), the fibrils formed by 1,7-DTPEPBI molecules in a water/THF mixture with a f_W of 40% (B). (C) and (D) are the confocal fluorescence images corresponding to the microstructures shown in (A) and (B), respectively. Images showing the waveguide properties of the microcrystals (E) and fibrils (F), some brighter spots are indicated by arrows. Excitation wavelength is 488 nm. Amplification factor for all images (A), (B), (C) and (D) is 40.

prism-like microcrystals and fibrils display brighter red light spots at the tips in comparison with the emission from the side (Fig. 6E, F, S15 and S16†). Meanwhile, the fluorescence contrast between the tips and the middle exhibits a dependence on the specific ratio of diameter and length of the microstructures; a larger specific ratio corresponds to better performance (Fig. S15A to S15D†). Besides, the waveguide performance relies on the surface properties of the microcrystals, and the microcrystals with higher surface quality exhibit better guiding behaviour (Fig. S16†). Moreover, the waveguide performance also depends on the morphology of the microcrystals. The needle-like crystals with sharp ends or the powder samples did not exhibit waveguide behaviour due to the non-uniform morphology (Fig. S17†) which dissipates the absorbed optical energy. These observations demonstrated primary characteristics of waveguides, implying DTPEPBIs could be potentially used as molecular materials for optical devices.[15,16]

Concluding remarks

In summary, two novel isomeric PBI derivatives, *i.e.* 1,6-/1,7-DTPEPBI, have been synthesized, clearly separated and characterized. Both 1,6- and 1,7-DTPEPBI demonstrate evident AIE behaviour. For 1,7-DTPEPBI, the fluorescence quantum efficiency of the solid film ($\Phi_{F,solid} = 6.3\%$) is 90 times that of the dilute solution ($\Phi_{F,solut} = 0.07\%$). The successful transition of the PBIs from ACQ to AIE behaviour, together with our previous achievements on other fluorogens such as pyrene, anthracene, and naphthalene, indicates that decoration of ACQ fluorogens with TPE moieties is an effective strategy to construct novel AIE active materials. In the present work, linking two TPE moieties to the 1,7-positions of the PBI core results in little change of the electronic structure, thus 1,7-DTPEPBI exhibits electrochemical behaviour of a typical n-type organic semiconductor. On the other hand, such a decoration results in an evident red-shift of fluorescence spectrum. For the solids of 1,7-DTPEPBI formed in water/THF mixed solutions, the spectral shifts are both around 120 nm (from 546 to 668 nm), indicating that the two PBI derivatives are red-emission materials. The evident red-shift is partially ascribed to the planar configuration of the perylene core. It is an interesting observation that the attachment of bulky and twisted TPE moieties onto the PBI core has not interrupted the formation of ordered assemblies and well-defined 1D microstructures (fibers, wires and rods) have been obtained in different non-solvent/solvent (water/THF, methanol/DCM, hexane/DCM, methanol/dioxane) mixtures. These microstructures emit bright red fluorescence and demonstrate waveguide activity. Based on the advantages arising from the combination of classical PBI fluorogens and AIE active TPE moieties, we expect the present strategy could provide a generic route towards novel and advanced fluorescent materials and these materials may find versatile applications in high-tech fields.

Experimental

Chemicals and materials

All the chemicals used were purchased from Acros or Alfa, unless specifically stated. Bromine was purchased from Alladin. THF was distilled under nitrogen from sodium benzophenone ketyl immediately prior to use. All other solvents were of analytical grade and were purified using standard methods.

Instrumentations

^{1}H and ^{13}C NMR spectra were measured on a Bruker AV 400 or 500 spectrometer in $CDCl_3$. UV spectra were measured on a Milton Roy Spectronic 3000 Array spectrophotometer. Fluorescence spectra were recorded on a Perkin-Elmer LS 55 spectrofluorometer. Φ_F values were estimated using Rhodamine B in ethanol ($\Phi_F = 70\%$) as standard. The absorbance of the solutions was kept between 0.04 and 0.06 to avoid the internal filter effect. Elemental analysis was performed on a ThermoFinnigan Flash EA1112. Scanning electron microscope (SEM) images were taken on a JSM-5510 scanning electron microscopy. Fluorescence micrographs were taken on an inverted fluorescence microscope (Nikon Eclipse TE2000-U). CHI-600 Electrochemical Workstation using 0.1 M n-Bu_4NPF_6 in dichloromethane as supporting electrolyte. The working and counter electrodes were platinum wires, and the reference electrode was $Hg/HgCl_2$. The polarized optical images were observed with an Olympus BX 60 polarized optical microscope (POM).

Synthesis of 1,6-dibromo-3,4:9,10-tetracarboxylic perylene dianhydride and 1,7-dibromo-3,4:9,10-tetracarboxylic perylene dianhydride

In a 250 mL three-necked round-bottom flask, perylene-3,4:9,10-tetracarboxylic dianhydride (4.0 g, 10.3 mmol) was added, and 100 mL concentrated sulfuric acid (98%) was added, then the mixture were stirred for18 h. Iodine (0.1 g, 0.4 mmol) was added to the mixture for an additional 5 h at 55 °C. Bromine (0.6 mL, 11.5 mmol) was added dropwise to the mixture over 0.5 h, and stirred for 24 h at 85 °C. After cooling to 40 °C, the excess bromine was eliminated by N_2. Then the mixture was poured into ice water, the precipitate was separated by filtration, and gave compound **2** (5.4 g, 96%). The crude product was not further purified for its poor solubility.

Synthesis of *N*,*N*′-dicyclohexyl-1,6/1,7-dibromo-3,4:9,10-tetracarboxylic perylene bisimide (1,6-/1,7-DBrPBI)

In a 250 mL two-necked round-bottom flask, the mixture of 1,7- and 1,6-dibromo-3,4:9,10-tetracarboxylic perylene dianhydride (2.9 g, 5.2 mmol), and 90 mL NMP were added, and the mixture were placed in a sonicator for 0.5 h. Then cyclohexylamine (2.4 mL, 20.8 mmol) and 10 mL acetic acid were added to the reaction mixture. The mixture was stirred for 24 h at 85 °C under N_2 atmosphere. After cooling to room temperature, ice water was added to the flask; then the mixture was poured into 600 mL water. The resulting precipitate was separated by filtration. The crude product was purified by a silica gel column using chloroform/petroleum ether (3 : 2 by volume) as eluent. A red solid was obtained in 62% yield (2.3 g). ^{1}H NMR (400 MHz, $CDCl_3$, δ): 9.45 (d, 2H), 8.85 (s, 2H), 8.65 (d, 2H), 5.00 (m, 2H), 2.54 (m, 4H), 1.93 (m, 4H), 1.76 (m, 6H), 1.47 (m, 4H), 1.35 (m, 2H); ^{13}C NMR (300 MHz, $CDCl_3$, δ): 163.5, 162.9, 138.1, 132.9, 132.8, 130.1, 129.4, 128.6, 127.2, 123.8, 123.5, 120.9, 54.5, 29.3, 26.7, 25.6.

Synthesis of *N*,*N*′-dicyclohexyl-1,6-/-1,7-di(4-(1,2,2-triphenyl) vinyl)phenyl-3,4:9,10-tetracarboxylic perylene bisimide (1,6-/ 1,7-DTPEPBI)

In a 250 mL two-necked round-bottom flask, the mixture of 1,6-DBrPBI and 1,7-DBrPBI (0.5 g, 0.7 mmol), TPVPBC (0.79 g, 2.1 mmol), and $Pd(PPh_3)_4$ (40 mg) were added. The flask was evacuated under vacuum and flushed with nitrogen three times. THF (80 mL) and 2 M Na_2CO_3 were injected into the flask. The mixture was refluxed for 48 h. After cooling to room temperature, the mixture was added to 80 mL water and extracted with DCM. The collected organic layer was dried over anhydrous magnesium sulfate. After solvent evaporation, the crude product was purified by a silica gel column using DCM/petroleum ether (2 : 3 by volume) as eluent, two bands could be seen. The first band afforded pure 1,6-DTPEPBI, and the second one afforded pure 1,7-DTPEPBI.

Characterization data of 1,7-DTPEPBI. A dark red solid was obtained in 45% yield (0.38 g). ^{1}H NMR (500 MHz, $CDCl_3$, δ): 8.51 (s, 2H), 8.14 (d, 2H), 7.77 (d, 2H), 7.06–7.30 (m, 38H), 5.01–5.06 (m, 2H), 2.53–2.61 (m, 4H), 1.91–1.93 (m, 4H), 1.75–1.77 (m, 6H), 1.49–1.52 (m, 4H), 1.37–1.42 (m, 2H); ^{13}C NMR (500 MHz, $CDCl_3$, δ): 163.9, 163.7, 144.5, 143.6, 143.4, 143.3, 142.0, 140.8, 140.1, 135.0, 134.5, 133.0, 132.2, 131.3, 129.9, 129.1, 128.4, 128.0, 127.9, 127.7, 127.6, 126.9, 126.7, 126.7, 122.7, 122.3, 53.9, 29.1, 26.5, 25.4. Anal. Calcd for $C_{88}H_{66}N_2O_4 \cdot 2H_2O$: C 84.45, H 5.64, N 2.24; found: C 84.36, H 5.79, N 2.18.

Characterization data of 1,6-DTPEPBI. A dark red solid was obtained in 12% yield (0.098 g). ^{1}H NMR (500 MHz, $CDCl_3$, δ): 8.50 (s, 2H), 8.17 (d, 2H), 7.78 (d, 2H), 7.06–7.31 (m, 38H), 5.02–5.06 (m, 2H), 2.53–2.61 (m, 4H), 1.89–1.94 (m, 4H), 1.76 (m, 6H), 1.45–1.51 (m, 4H), 1.34–4.38 (m, 2H); ^{13}C NMR (500 MHz, $CDCl_3$, δ): 164.2, 164.1, 144.6, 143.8, 143.7, 142.2, 140.8, 140.3, 135.3, 134.3, 133.4, 132.9, 131.6, 129.9, 129.6, 128.4, 128.3, 128.1, 127.9, 127.2, 126.9, 122.8, 122.7, 54.3, 54.1, 29.9, 29.4, 26.8, 25.7. Anal. Calcd for $C_{88}H_{66}N_2O_4 \cdot 2H_2O$: C 84.45, H 5.64, N 2.24; found: C 84.26, H 5.91, N 1.97.

Theoretical calculations

All calculations on the considered molecules were performed by using the Gaussian 09 program package.[17] The relative energies of the HOMO and LUMO levels were obtained from the computed results.

Acknowledgements

This work was supported from the National Science Foundation of China (21074113); the key project of the Ministry of Sci. & Technol. of China (2009CB623605), the Science Foundation of Zhejiang Province (Z4110056), the Research Grants Council of Hong Kong (603509, HKUST2/CRF/10, and 604711), the SRFI grant of HKUST (SRFI11SC03PG), the NSFC/RGC grant (N_HKUST620/11), the University Grants Committee of Hong Kong (AoE/P-03/08). B.Z.T. thanks the support from the Cao Guangbiao Foundation of Zhejiang University.

Notes and references

1 Examples of recent reviews. (*a*) X. W. Zhan, A. Facchetti, S. Barlow, T. J. Marks, M. A. Ratner, M. R. Wasielewski and S. R. Marder, *Adv. Mater.*, 2011, **23**, 268; (*b*) R. Bhosale, J. Misek, N. Sakai and S. Matile, *Chem. Soc. Rev.*, 2010, **39**, 138; (*c*) M. R. Wasielewski, *Acc. Chem. Res.*, 2009, **42**, 1910.

2 (*a*) B. J. Jung, N. J. Tremblay, M.-L. Yeh and H. E. Katz, *Chem. Mater.*, 2011, **23**, 568; (*b*) T. Weil, T. Vosch, J. Hofkens, K. Peneva and K. Müllen, *Angew. Chem., Int. Ed.*, 2010, **49**, 9068; (*c*) B. A. Jones, A. Facchetti, M. R. Wasielewski and T. J. Marks, *J. Am. Chem. Soc.*, 2007, **129**, 12529; (*d*) Z. S. An, J. S. Yu, S. C. Jones, S. Barlow, S. Yoo, B. Domercq, P. Prins, L. D. A. Siebbeles, B. Kippelen and S. R. Marder, *Adv. Mater.*, 2005, **17**, 2580.

3 (*a*) F. Würthner, T. E. Kaiser and C. R. Saha-Moller, *Angew. Chem., Int. Ed.*, 2011, **50**, 3376; (*b*) L. V. Malinovskii, D. Wenger and R. Haener, *Chem. Soc. Rev.*, 2010, **39**, 410; (*c*) S. Varghese, N. S. S. Kumar, A. Krishna, D. S. S. Rao, S. K. Prasad and S. Das, *Adv. Funct. Mater.*, 2009, **19**, 2064; (*d*) C. Hippius, I. H. M. van Stokkum, M. Gsanger, M. M. Groeneveld, R. M. Williams and F. Würthner, *J. Phys. Chem. C*, 2008, **112**, 2476.

4 (*a*) D. Gonzalez-Rodriguez and A. P. H. J. Schenning, *Chem. Mater.*, 2011, **23**, 310; (*b*) T. F. A. De Greef, M. M. J. Smulders, M. Wolffs, A. P. H. J. Schenning, R. P. Sijbesma and E. W. Meijer, *Chem. Rev.*, 2009, **109**, 5687; (*c*) J. E. Bullock, R. Carmieli, S. M. Mickley, J. Vura-Weis and M. R. Wasielewski, *J. Am. Chem. Soc.*, 2009, **131**, 11919; (*d*) L. Zang, Y. Che and J. S. Moore, *Acc. Chem. Res.*, 2008, **41**, 1596; (*e*) Z. J. Chen, V. Stepanenko, V. Dehm, P. Prins, L. D. A. Siebbeles, J. Seibt, P. Marquetand, V. Engel and F. Würthner, *Chem.–Eur. J.*, 2007, **13**, 436.

5 Y. Hong, J. W. Y. Lam and B. Z. Tang, *Chem. Commun.*, 2009, 4332.

6 (*a*) Y. Che, X. Yang, K. Balakrishnan, J. Zuo and L. Zang, *Chem. Mater.*, 2009, **21**, 2930; (*b*) M. K. R. Fischer, T. E. Kaiser, F. Würthner and P. Bauerle, *J. Mater. Chem.*, 2009, **19**, 1129; (*c*) J. Qu, J. Zhang, A. C. Grimsdale, K. Müllen, F. Jaiser, X. Yang and D. Neher, *Macromolecules*, 2004, **37**, 8297.

7 (*a*) J. Luo, Z. Xie, J. W. Y. Lam, L. Cheng, H. Chen, C. Qiu, H. S. Kwok, X. Zhan, Y. Liu, D. Zhu and B. Z. Tang, *Chem. Commun.*, 2001, 1740; (*b*) Y. Dong, J. W. Y. Lam, A. Qin, Z. Li, J. Sun, H. H. Y. Sung, I. D. Williams and B. Z. Tang, *Chem. Commun.*, 2007, 40; (*c*) B. Z. Tang, Y. N. Hong and J. W. Y. Lam, *Chem. Commun.*, 2009, 4332.

8 Y. Hong, J. W. Y. Lam and B. Z. Tang, *Chem. Soc. Rev.*, 2011, **40**, 5361.

9 (*a*) Z. J. Zhao, P. Lu, J. W. Y. Lam, Z. M. Wang, C. Y. K. Chan, H. H. Y. Sung, I. D. Williams, Y. G. Ma and B. Z. Tang, *Chem. Sci.*, 2011, **2**, 672; (*b*) Z. J. Zhao, S. M. Chen, J. W. Y. Lam, Z. M. Wang, P. Lu, F. Mahtab, H. H. Y. Sung, I. D. Williams, Y. G. Ma, H. S. Kwok and B. Z. Tang, *J. Mater. Chem.*, 2011, **21**, 7210; (*c*) Z. Zhao, S. Chen, J. W. Y. Lam, P. Lu, Y. Zhong, K. S. Wong, H. S. Kwok and B. Z. Tang, *Chem. Commun.*, 2010, **46**, 2221.

10 B. A. Jones, M. J. Ahrens, M. H. Yoon, A. Facchetti, T. J. Marks and M. R. Wasielewski, *Angew. Chem., Int. Ed.*, 2004, **43**, 6363.

11 For example: (*a*) N. V. Handa, K. D. Mendoza and L. D. Shirtcliff, *Org. Lett.*, 2011, **13**, 4724; (*b*) R. K. Dubey, A. Efimov and H. Lemmetyinen, *Chem. Mater.*, 2010, **23**, 778; (*c*) L. Fan, Y. Xu and H. Tian, *Tetrahedron Lett.*, 2005, **46**, 4443.

12 (*a*) H. X. Wu, L. Xue, Y. Shi, Y. L. Chen and X. Y. Li, *Langmuir*, 2011, **27**, 3074; (*b*) C. Huang, S. Barlow and S. R. Marder, *J. Org. Chem.*, 2011, **76**, 2386; (*c*) J. Feng, B. Liang, D. Wang, H. Wu, L. Xue and X. Li, *Langmuir*, 2008, **24**, 11209; (*d*) J. M. Giaimo, J. V. Lockard, L. E. Sinks, A. M. Scott, T. M. Wilson and M. R. Wasielewski, *J. Phys. Chem. A*, 2008, **112**, 2322; (*e*) S. W. Thomas, G. D. Joly and T. M. Swager, *Chem. Rev.*, 2007, **107**, 1339.

13 (*a*) S. Ghosh, X.-Q. Li, V. Stepanenko and F. Würthner, *Chem.–Eur. J.*, 2008, **14**, 11343; (*b*) S. Yagai and J. Photochem., *J. Photochem. Photobiol., C*, 2006, **7**, 164; (*c*) Y. Che, X. Yang, S. Loser and L. Zang, *Nano Lett.*, 2008, **8**, 2219.

14 (*a*) Z. Chen, U. Baumeister, C. Tschierske and F. Würthner, *Chem.–Eur. J.*, 2007, **13**, 450; (*b*) X. Q. Li, X. Zhang, S. Ghosh and F. Würthner, *Chem.–Eur. J.*, 2008, **14**, 8074; (*c*) S. Ghosh, X. Q. Li, V. Stepanenko and F. Würthner, *Chem.–Eur. J.*, 2008, **14**, 11343.

15 (*a*) K. Takazawa, *Chem. Mater.*, 2007, **19**, 5293; (*b*) K. Takazawa, Y. Kitahama, Y. Kimura and G. Kido, *Nano Lett.*, 2005, **5**, 1293.
16 X. Wang, Y. Zhou, T. Lei, N. Hu, E. Q. Chen and J. Pei, *Chem. Mater.*, 2010, **22**, 3735.
17 *Gaussian 09 (Revision A.02)*, M. J. Frisch, G. W. Trucks, H. B. Schlegel, G. E. Scuseria, M. A. Robb, J. R. Cheeseman, G. Scalmani, V. Barone, B. Mennucci, G. A. Petersson, H. Nakatsuji, M. Caricato, X. Li, H. P. Hratchian, A. F. Izmaylov, J. Bloino, G. Zheng, J. L. Sonnenberg, M. Hada, M. Ehara, K. Toyota, R. Fukuda, J. Hasegawa, M. Ishida, T. Nakajima, Y. Honda, O. Kitao, H. Nakai, T. Vreven, J. A. Montgomery, J. E. Peralta, Jr., F. Ogliaro, M. Bearpark, J. J. Heyd, E. Brothers, K. N. Kudin, V. N. Staroverov, R. Kobayashi, J. Normand, K. Raghavachari, A. Rendell, J. C. Burant, S. S. Iyengar, J. Tomasi, M. Cossi, N. Rega, J. M. Millam, M. Klene, J. E. Knox, J. B. Cross, V. Bakken, C. Adamo, J. Jaramillo, R. Gomperts, R. E. Stratmann, O. Yazyev, A. J. Austin, R. Cammi, C. Pomelli, J. W. Ochterski, R. L. Martin, K. Morokuma, V. G. Zakrzewski, G. A. Voth, P. Salvador, J. J. Dannenberg, S. Dapprich, A. D. Daniels, O. Farkas, J. B. Foresman, J. V. Ortiz, J. Cioslowski and D. J. Fox, Gaussian, Inc., Wallingford CT, 2009; K. Tamao, M. Uchida, T. Izaumizawa, K. Furukawa and S. Yamaguchi, *J. Am. Chem. Soc.*, 1996, **118**, 11974.

